

System Level Hybrid Functional and Power Modeling Methodology to Extend The Longevity of Implantable Seizure Controllers

Sunhee Kim, Seungdo Jeong

Abstract

Background/Objectives: An implantable seizure controller needs a system level model to predict power generation and consumption as well as function because it has a limited power source.

Methods/Statistical analysis: The targeted system is divided into several sub-blocks according to functions. Each sub-block is redefined in respect of energy. They have information about both their functional operation and role of energy. This model is developed in Simulink/Matlab environment that supports multi-domain components and customizable libraries efficiently. It was examined for an implantable seizure controller using data with seizure and non-seizure.

Findings: Most system models for power estimation have usually considered physical-level and instruction-level models based on processors. They are used to measure power consumption of system while programs are running. Few system level architectures have been presented that consider both power consumption and power generation. Because a closed loop seizure controller may be implanted with limited power sources, it needs to be designed with consideration for power consumption and generation together. The proposed system level modeling methodology supports power generation and consumption description, and a dynamic power management scheme in a single domain as well as functional behavior check. It enables system designers to consider system specifications within a given power budget at the early stage of design.

Improvements/Applications: This hybrid function and power modeling methodology can be applied to a system with a limited power source, such as implantable medical devices and sensor network modules.

Keywords: power management, seizure controller, implantable biomedical device, power modeling, system-level design, system modeling

I. INTRODUCTION

Epilepsy disorders affect more than 60 million people around the world and an estimated 2.4 million new patients are diagnosed each year¹⁻³. An epileptic seizure is one of the most common signs of epilepsy⁴⁻⁵. About 75% seizures are sufficiently controllable with antiepileptic drug medications and respective epilepsy surgery. Some seizures do not

respond to these conventional treatments⁵⁻⁶. Brain stimulation has recently been considered as an optional therapy.

Implantable seizure controllers with brain stimulation is built into a closed loop device for higher efficiency than an open loop device that stimulates according to the schedule regardless of seizure occurrences⁷. A closed loop seizure controller continuously monitors an intracranial electroencephalography (icEEG) and extracts the characteristic features of seizures from the icEEG. When it detects the occurrence of the seizure, it generates stimulation signals to normalize the brain activity in real time. Seizure detection performance is one of the most important aspects of a closed-loop seizure controller.

Implantable devices including a closed loop seizure controller usually consist of multi-domain components such as analog devices, digital devices, wireless communication devices, and power sources⁸. Because each component has its specific design environment, implantable devices can be integrated with sub-components that are designed separately. However, an effective system level design is required from the beginning of a design. Specifically, the implantable devices usually have batteries as their power source. Battery life, such as the time of one operating cycle on a full charge and the number of charge cycles, is limited. An implanted device must be replaced surgically due to its dead batteries. This can lead to physical pain, psychological distress and economic burden for patients⁹. The system level model for the implantable device needs to be able to estimate power distribution as well as functionality in order to extend the longevity of the device under a given power budget.

System models for power estimation have been proposed. They usually consider physical-level and instruction-level models for processors and measure power consumption of system while programs are running¹⁰⁻¹⁴. However, few system level architectures have been presented that consider both power consumption and power generation⁸. Therefore, we propose a system level modeling methodology that supports functional behavior check, power generation/consumption description, and a dynamic power management scheme in a single domain.

This paper is organized as follows. Section 2 describes the system level modeling methodology to predict both function and power. In addition, the implantable closed loop seizure controller is

Revised Manuscript Received on May 22, 2019.

¹Sunhee Kim, Department of System Semiconductor Engineering, Sangmyung University, 31, Sangmyungdae-gil, Dongnam-gu, Cheonan-si, Chungcheongnam-do, Korea

²Seungdo Jeong, Corresponding author, Department of Smart Information and Telecommunication Engineering, Sangmyung University, 31, Sangmyungdae-gil, Dongnam-gu, Cheonan-si, Chungcheongnam-do, Korea
happyshkim@smu.ac.kr¹, sjeong@smu.ac.kr²



discussed to demonstrate the method of fabricating the proposed system level model and utilizing the designed model. Section 3 describes the simulation results and the conclusions are given in Section 4.

II. MATERIALS AND METHODS

2.1. Hybrid model building methodology

This section describes our methodology for building a system level hybrid functional and power model. It uses the power consumption of each functional block according to its operating modes. The total power consumption is estimated based on the linear regression.

System designers generally research and understand the function and performance requirements of an entire system, and its diverse implementation aspects. When designers divide a targeted system into several sub-blocks, typically the sub-blocks are grouped by their signal domains: an analog signal processing block, a digital signal processing block, a wireless signal processing block, a power block and so on. Then, each sub-block needs to be specified according to various factors, such as its function, input/output signals, and target performance. Because sub-blocks have different performances depending on how they are implemented, system designers need to set specifications of sub-blocks based on their design environments.

After processed by the general method described above, each sub-block is redefined in respect of energy as an energy source, an energy consumer, and a power manager. An energy source generates/stores energy and supplies it to energy consumers at the dictation of a power manager. The energy source defines the amount of energy that can be stored, the amount of energy already stored, and the rate at which energy can be generated. An energy consumer knows the amount of power consumed depending on its operating mode and the rate at which it requires energy. A power manager predicts operations of the whole system and the consequential power consumption and distributes energy to each sub-block appropriately. Our power managing strategies are as follows.

- 1) The power manager selects an operating mode of energy consumer blocks.
- 2) It also selects the methods to change the operating mode.
- 3) The operating mode of the energy consumer blocks can be changed according to the expected system operations, remaining energy, and their priorities determined by the power manager.
- 4) The power request and distribution are processed based on an event-driven method.

System level designers need to set design targets and simulate repeatedly to get an optimum power management strategy that keeps the system doing under limited power conditions. For example, a seizure controller is needed to determine whether or not some of the monitoring and/or stimulating channels will be off, or whether or not the amplifier's gain will be increased. Consequently, this model gives the designers rapid feedback on their design decisions.

We used Matlab/Simulink developed by Mathworks. Matlab is a numerical computing environment¹⁵. Simulink, which is an additional package of Matlab, is a graphical block diagramming environment for multi-domain simulation and model-based design. Simulink supports user defined block libraries and can be integrated with a Matlab environment¹⁶. Therefore, an integrated Matlab/Simulink environment is appropriate for system level modeling with multi-domain components and customizable libraries.

The next section describes the design process of our proposed system level modeling for an implantable closed loop seizure controller.

2.2. Functional and Power Model Design

As shown in figure1, a closed loop seizure controller consists of a MonitoringElectrode, an AnalogFrontEnd, a SeizureDetector, a Stimulator, a StimulatingElectrode, a WirelessCommunicator, a PowerGenerator and a PowerManager. The Monitoring Electrode, the AnalogFrontEnd, the SeizureDetector, the Stimulator, the StimulatingElectrode and the WirelessCommunicator are labeled as an energy consumer in terms of energy. The PowerGenerator and the PowerManager are classified as an energy source and a power manager, respectively.

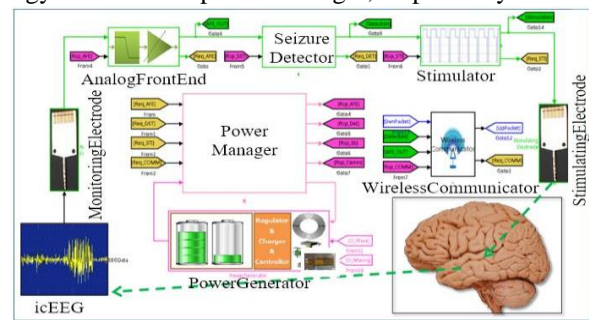


Figure 1. Top block of a system level model for a closed-loop seizure controller.

The icEEG is a type of test-bench block that provides input signals. The signals include both seizure (between 0 s and 300 s) and non-seizure (between 300 s and 600 s).

2.2.1. MonitoringElectrode and StimulatingElectrode

The MonitoringElectrode and the StimulatingElectrode transfer icEEG signals to the AnalogFrontEnd and stimulation signals to the brain, respectively. They are defined as a signal attenuator. Although they are classified as energy consumers, they do not request power.

2.2.2. AnalogFrontEnd

The AnalogFrontEnd consists of a signal processing block and a power requesting block. The signal processing block amplifies the icEEG signals, enhances seizure-occurring frequency components from the signals, and converts them into digital data. In addition, it generates a detection enable signal to wake up a detector when the signal reaches above a threshold, V_{th_enSD} .

The AnalogFrontEnd has the signal processing block with N-channels. Each channel is composed of an amplifier, a filter, an ADC and a signal detector to enable the



seizure detector. A multi-channel device can be implemented with either a multiplexed ADC or an individual ADC^{17,18}. We assumed an individual ADC structure.

The AnalogFrontEnd supports the subsequent operating modes. Basically, it has a power-off mode and active modes. The active modes are classified according to performance parameters: an ADC sampling frequency, an ADC resolution, and an amplifier gain¹⁸⁻²⁰. The power consumption at each mode differs. The sampling frequency and the resolution of an ADC depend on a seizure detection algorithm in the case of a seizure controller. This model assumes that the sampling frequency is fixed. We set a 3-level amplifier gain. The power consumption for one channel including an 8-bit ADC is 50 uW, 200 uW, and 400 uW according to the gains with reference to [18, 19]. Also, we assume that if the resolution is increased to 12 bits, the power consumption also increases by 5 uW. Therefore, the AnalogFrontEnd supports seven operating modes. If it activates N channels, the power consumption increases linearly N times. Because the AnalogFrontEnd always operates regardless of seizure occurrences, it requests power periodically.

2.2.3. Seizure Detector

The SeizureDetector, similar to the AnalogFrontEnd, consists of a signal processing block and a power requesting block. The signal processing block is composed of an N-to-1 multiplexer and a processor for seizure detection algorithm execution. To process N-channel neural signals, seizure detectors can have several structures such as N detectors in parallel, one detector in a time-division scheme, and one detector for a selected channel²¹⁻²³. Because we set the seizure detector to process one channel with the earliest detection enable signal, an N-to-1 multiplexer is needed.

The performance and power consumption of seizure detectors vary depending on the seizure detection algorithm used^{22,24}. This model adopts a Generic Osorio Frei Algorithm (GOFA)²⁵⁻²⁸.

The SeizureDetector remains in power-off mode until it is enabled by the AnalogFrontEnd. The SeizureDetector immediately requests the power, and then processes the detection algorithm after receiving the power. When a seizure occurrence is detected, the block sends an alarm signal and returns to the power-off mode. The GOFA can be implemented by using either a general processor or a specific circuit. Based on the 12-bit GOFA specific system in [26], we set two active modes with 10 uW at 12-bit processing and 9 uW at 8-bit processing.

A false positive (FP) is a result that indicates a seizure occurs, when it actually does not occur. A FP rate depends on the parameters of the algorithm and affects the power consumption of the system during a run time. If a FP alarm is sent, a stimulator operates and power is consumed unnecessarily. If the SeizureDetector adjusts the relevant parameters to decrease the rate of FP, an error can occur whereby a seizure occurrence is missed. Therefore, we add a performance parameter to control the power consumption.

A Simulink model for the SeizureDetector consists of the seizure detector processor and the power requesting block. The seizure detector processor is defined with Matlab function blocks, which enable the Matlab codes executed in a Simulink model, due to the complexity of the detection algorithm.

2.2.4. Stimulator

As an energy consumer, the Stimulator consists of a signal processing block and a power requesting block. The signal processing block generates electrical stimulation signals to suppress seizures. It has M channels and the number of enabled channels is determined by the PowerManager.

When the SeizureDetector triggers a seizure alarm, the operating mode of the Stimulator is changed from a power-off mode to an active mode. Then, the Stimulator requests power from the PowerManager and generates stimulation signals after receiving the power.

The power consumption of this block varies a few hundred nW to a few dozen mW according to the magnitude and shape of the stimulation signals, the duration of stimulation, and so on^{7,23,29}. We apply three active modes with each power consumption, 600 uW, 3 mW, and 15 mW, respectively, for one channel with reference to [7]. If the Stimulator uses M channels, the total power consumption of the SeizureDetector increases linearly M times.

2.2.5. WirelessCommunicator

The WirelessCommunicator also consists of a signal processing block and a power requesting block. The WirelessCommunicator is used to report the status of the system to an external host and to update the system by the external host.

We decide that the block consumes 2 mW at the transmitting mode and 2.5 mW at the receiving mode using a [27]. Because the WirelessCommunicator is not a main functional block, we assume this block operates once a day.

2.2.6. PowerGenerator

The PowerGenerator is a power source in terms of energy. It is composed of an energy source, an AC-DC converter, a charger, a regulator, and rechargeable batteries as shown in figure 2. We consider a wireless power transfer (WPT) and a vibration-driven energy harvester. These energy sources generate an AC, which is converted to a DC through an AC-DC converter. The charger charges the battery while the converted DC ranges between maximum and minimum thresholds to protect the battery. The regulator changes the supply voltage level from a battery voltage to a voltage required by loads. The energy efficiencies of the AC-DC converter, the charger, and the regulator are all set at 80% according to [30-32], and [33, 34], respectively.

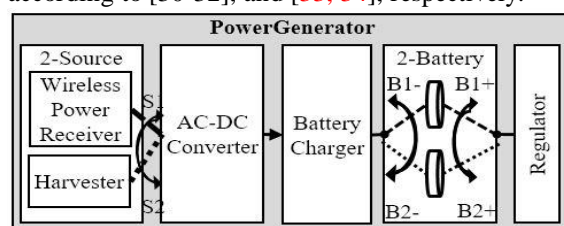


Figure 2. Block diagram of the PowerGenerator

This PowerGenerator includes two 4 V 2.2 mA·h thin-film micro-energy cells³⁵. One is used for the load and the other is charged alternately. When the PowerManager inquiries about the usable energy quantity, the PowerGenerator offers the total energy stored in the two cells. When the PowerManager requests power, the PowerGenerator provides energy from the load-used battery first. If the energy of the load-used battery is zero and the energy of the charged battery is not zero, the PowerGenerator exchanges the roles of these batteries.

2.2.7. PowerManager

Whenever energy consumers (the AnalogFrontEnd, the SeizureDetector, the Stimulator, and the WirelessCommunicator) occur power request events, the PowerManager checks the remaining energy and current states, decides the appropriate operating modes of each sub-block, and distributes energy.

Strategies and assumptions for power management are as follows. This system level model manages power on a daily basis. While the patient with an implantable seizure controller sleeps, two batteries inside it are fully charged through a WPT. The PowerManager measures the time duration of WPT charging, Tcharged. When the battery charging is finished, the PowerManager restarts in order that the system can operate properly with two charged batteries for at least (24-hours – Tcharged), Tremaining_init. While the patient is moving, the vibration-driven harvester generates energy intermittently. The occurrence of seizures is expected twice during the period of Tremaining_init.

Figure 3 shows the on-off status of each block according to function. The AnalogFrontEnd alone operates until it enables the SeizureDetector. While the SeizureDetector applies the detection algorithm, both the AnalogFrontEnd and the SeizureDetector operate. If a seizure occurrence is not detected, only the SeizureDetector returns to its off mode. If the SeizureDetector decides a seizure occurrence, only the Stimulator operates to suppress the seizure. The AnalogFrontEnd restarts monitoring after the stimulation is finished.

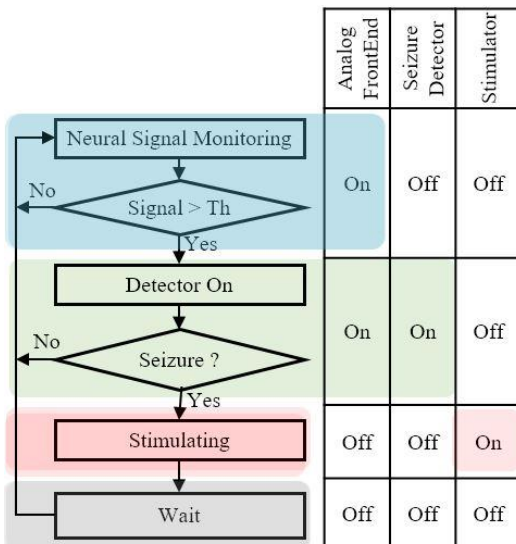


Figure 3. Flowchart of on-off status of each block according to function

Two flowcharts, as shown in figure 4 and figure 5, summarize the overall power managing process. The PowerManager is on standby until it receives a power request, as shown in figure 4. The AnalogFrontEnd requests power periodically, while the Detector and the Stimulator suddenly request power on special occasions. Therefore, when power is requested by the AnalogFrontEnd, the PowerManager updates the operating modes of each energy consumer and then distributes the energy according to the new selected operating mode. When the SeizureDetector or the Stimulator requests power, the PowerManager distributes power based on the currently set mode and then updates the operating modes. If the Stimulator requests power again within a certain time threshold, Tth_sti, after its last request, the PowerManager can allow more power within possible power budgets. When power is requested by the WirelessCommunicator, the PowerManager checks the current states. If WPT charging is on and the charged energy quantity of one battery is more than half of the full capacity, the PowerManager distributes power to the WirelessCommunicator.

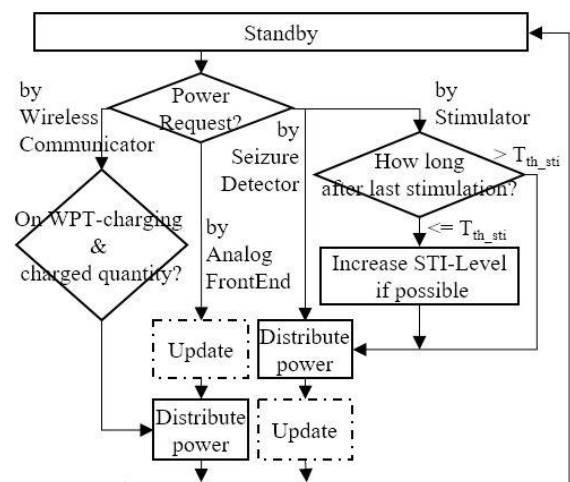


Figure 4. Flowchart of power managing process.

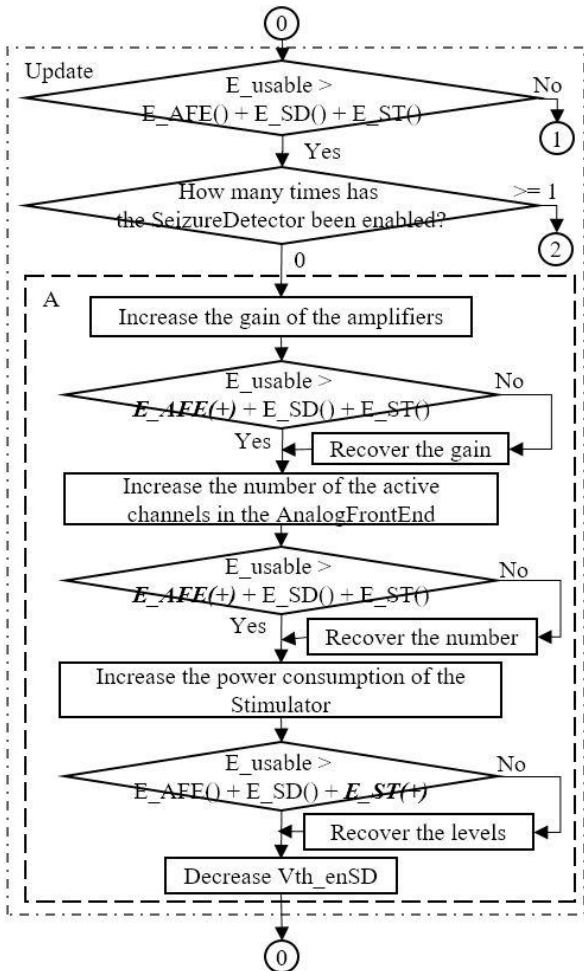


Figure 5.(a)

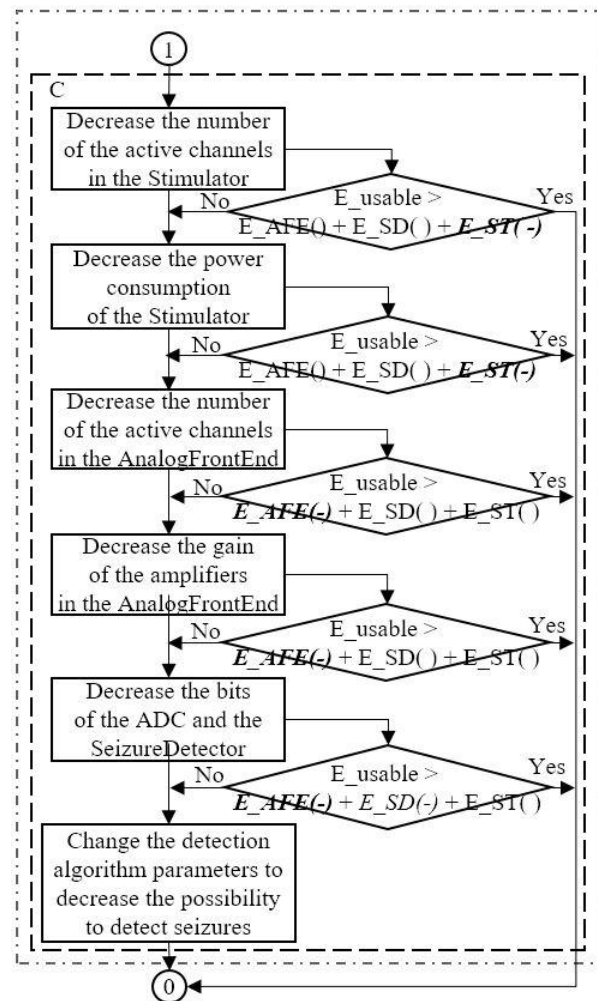


Figure 5. (c)

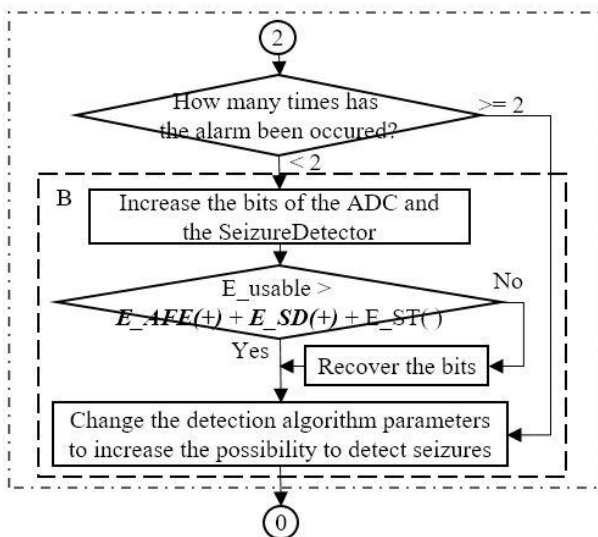


Figure 5.(b)

Figure 5. Flowchart of operating mode updating process, (a) the case of increasing power consumption, (b) the case of changing the detection algorithm parameters, and (c) the case of decreasing power consumption.

The PowerManager computes the following equation to update the power level as shown in figure 5.

$$E_{usable} \geq E_{AFE}(afe_mode, N, T_{remaining}) + E_{SD}(sd_mode, C_{enable}) + E_{ST}(st_mode, M, C_{enable}) \quad (1)$$

where E_{usable} is the stored energy in the batteries. E_{AFE} , E_{SD} , and E_{ST} are the expected energy requested by the AnalogFrontEnd, the SeizureDetector, and the Stimulator, respectively. E_{AFE} is calculated with the power related parameters of the AnalogFrontEnd: the operating mode of the AnalogFrontEnd (afe_mode), the number of AFE channels (N), and the estimated time until the next WPT charging ($T_{remaining}$). E_{SD} is calculated by using the power related parameters of the SeizureDetector: operating mode of the SeizureDetector (sd_mode) and the number of expected seizure occurrences until the next WPT charging (C_{enable}). E_{ST} is calculated with the power related parameters of the Stimulator: operating mode of the Stimulator (st_mode), the number of stimulating channels (M), and C_{enable} . During WPT charging, $T_{remainig}$



is set at 1h and C_enable is set 1.

If (1) is satisfied and no detector enable signal occurs (case A in figure 5(a)), the PowerManager considers increasing the power consumption according to the following orders.

- a) Increase the gain of the amplifiers in the AnalogFrontEnd
 - b) Increase the number of active channels in the AnalogFrontEnd
 - c) Increase the power consumption of the Stimulator
 - d) Decrease the threshold voltage, Vth_enSD, to wake up the SeizureDetector,
- and if (1) is satisfied after applying the conditions at each step, the PowerManager changes the operating modes into the satisfied modes.

If (1) is satisfied and less than 2 detection alarms have occurred (case B in figure 5(b)), the PowerManager changes the detection algorithm parameters to increase the possibility to detect seizures, and then checks whether (1) is satisfied after increasing the bits of the ADC and the SeizureDetector.

If E_usable is less than the sum (case C in figure 5(c)), the PowerManager decreases the power consumption according to the following orders.

- a) Decrease the number of the active channels in the Stimulator
- b) Decrease the power consumption of the Stimulator
- c) Decrease the number of active channels in the AnalogFrontEnd
- d) Decrease the gain of the amplifiers in the AnalogFrontEnd
- e) Decrease the bits of the ADC and the SeizureDetector
- f) Change the detection algorithm parameters to decrease the FP rate

and if (1) is not satisfied after applying conditions at each step, transit to the next step.

Figure 6 shows a Simulink model for the PowerManager. The on-off status managing in figure 3 is implemented using a Chart block (a block A), which is a graphical representation of a finite stat machine. The power managing process in figure 4 and figure 5 are modeled with a Matlab function block (block B).

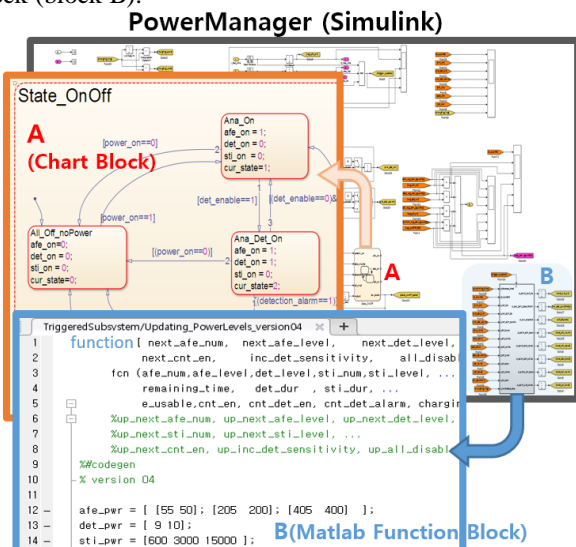


Figure 6. PowerManager Model

III. RESULTS AND DISCUSSION

3.1. Function simulation

Figure 7 and figure 8 show the function simulation results including signals of the icEEG, the SeizureDetector, and the Stimulator. As shown in figure 7, the SeizureDetector detected seizure occurrences (figure 7(b)) in the icEEG (figure 7(a)) and the Stimulator generated stimulation signals on each occasion (figure 7(c)). This simulation did not reflect the case in which a seizure was suppressed by an electrical stimulation. Therefore, a detection alarm occurred three times during one seizure.

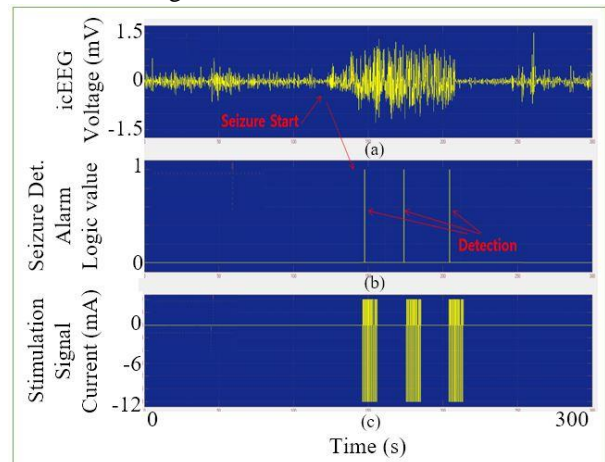


Figure 7. Function simulation results: case 1, (a) output of the icEEG, (b) output of the SeizureDetector, and (c) output of the Stimulator

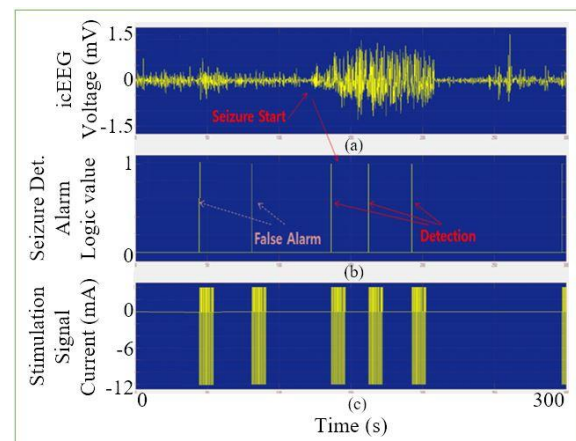


Figure 8. Function simulation results with the changed detection performance parameters: case 2, (a) output of the icEEG, (b) output of the SeizureDetector, and (c) output of the Stimulator.

In the case of figure 8, the same icEEG data but different detection performance parameters were used, which were set as lower threshold values to determine the seizure occurrence. Therefore, two false alarms occurred (figure 8(b)), which increased the number of unnecessary stimulation operations (figure 8(c)) and the consequential unnecessary energy consumption.

3.2. Power managing simulation



Figure 9 shows the power managing simulation results that indicate the distribution of energy during one day. The WPT supply energy from 0:00 hours for 6 hours. Two batteries were charged fully within about 1 hour (figure 9(a)) and were replenished as used energy over the next 5 hours. The WirelessCommunicator requested power once during WPC charging (figure 9(b)). The AnalogFrontEnd periodically requested power to monitor continuously icEEG (figure 9(c)). While two batteries were almost fully charged, two channels of the AnalogFrontEnd were used and their amplifiers were set at the second level gain. Then, the gain was decreased to the third level. After about 14:00 hours, the gain was changed according to the remaining energy quantity. The SeizureDetector was activated the four times (figure 9(d)). It decided that only two out of four irregular signals were seizure occurrences (figure 9(e)). Stimulator generated the second-level stimulation signals because the first seizure occurred and remained energy was sufficient. However, at about 19:30 hours, the stimulation signals decreased (figure 9(e)).

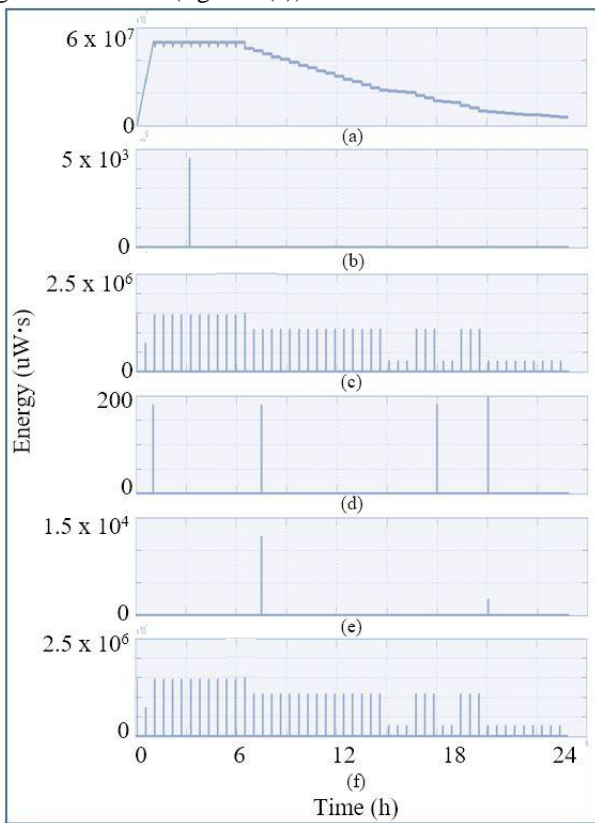


Figure 9. Power managing simulation results: case 1, (a) stored energy in batteries, (b) energy distributed to the WirelessCommunicator, (c) energy distributed to the AnalogFrontEnd, (d) energy distributed to the SeizureDetector, and (e) energy distributed to the Stimulator.

Figure 9(f) shows the sum of energy consumed by each sub-blocks. Compared with the sum of energy (figure 9(f)), the consumed energy by the AnalogFrontEnd accounted for almost all energy. Therefore, decreasing power consumption of the AnalogFrontEnd (figure 9(c)) is very important to assure an implantable closed loop seizure controller stability.

We changed our power managing strategy for the case of insufficient energy. We planned for each sub-block to

decrease its power consumption in the following order: the Stimulator, the AnalogFrontEnd, and the SeizureDetector. Since the AnalogFrontEnd consumed considerably more energy than the Stimulator, we changed the order of the Stimulator and the AnalogFrontEnd.

For the above simulation shown in figure 9, the power consumption of the Stimulator and the AnalogFrontEnd was lowered at about 14:00 hours. Therefore, the second stimulation signals were smaller than the first stimulation signals. Figure 10 shows the power managing simulation results with the new strategy. At about 14:00 hours, only the AnalogFrontEnd showed a decreased power consumption level (figure 10(c)). Therefore, the distributed power quantity for the second stimulation was the same as that of the distributed power quantity for the first stimulation (figure 10(e)). Based on the simulation results shown in figure 7-10, system level designers can analyze and redesign their target systems and dynamic power managing strategies by using the designed system level model.

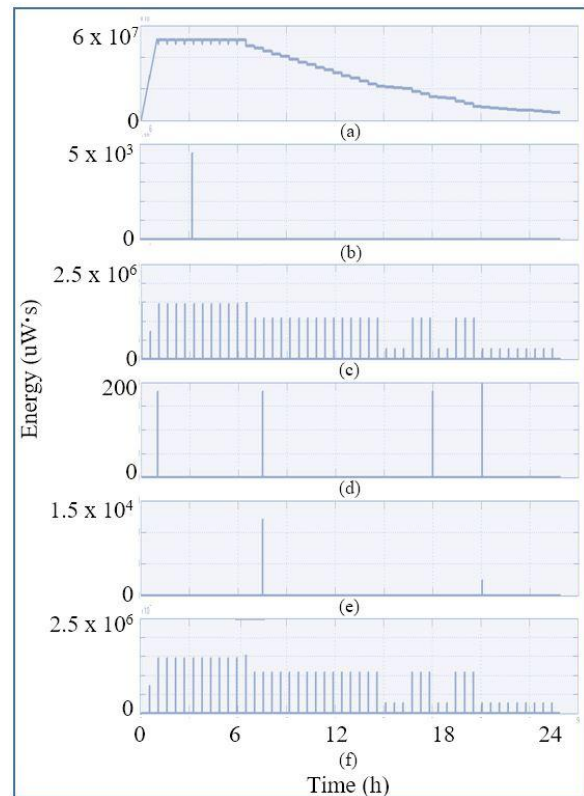


Figure 10. Power managing simulation results with the changed strategy: case 2, (a) stored energy in batteries, (b) energy distributed to the WirelessCommunicator, (c) energy distributed to the AnalogFrontEnd, (d) energy distributed to the SeizureDetector, and (e) energy distributed to the Stimulator.

Figure 11 shows the simulation results for the battery control over 24 hours. Figure 11(a) shows the external energy received by WPT, which was supplied for the first 6 hours, and the external energy received by the harvester, which was supplied twice. The stored energy (figure 11(b)) is the sum of the stored energy in battery 1 (figure 11(d)) and battery 2 (figure 11(e)). Initially, the battery mode was 0, which means battery 1 was charged and battery 2 was empty. In

this case, the system was powered off. As shown in the magnified images of figure 11(c), 11(d), and 11(e), the battery mode was changed to 1, which means battery 1 was used as a power supply and battery 2 was charged. The changing event occurred at about 10 min when battery 1 was charged up to 10%, rather than 100%, of the maximum capacity of the battery. When the power was requested at 0.5 h, battery 1 was almost empty and the battery mode was changed to 3, which means battery 1 was charged and battery 2 was used. The battery mode returned to 1 at about 3 o'clock when battery 1 was fully charged. After about 11 h, the battery mode stayed 3.

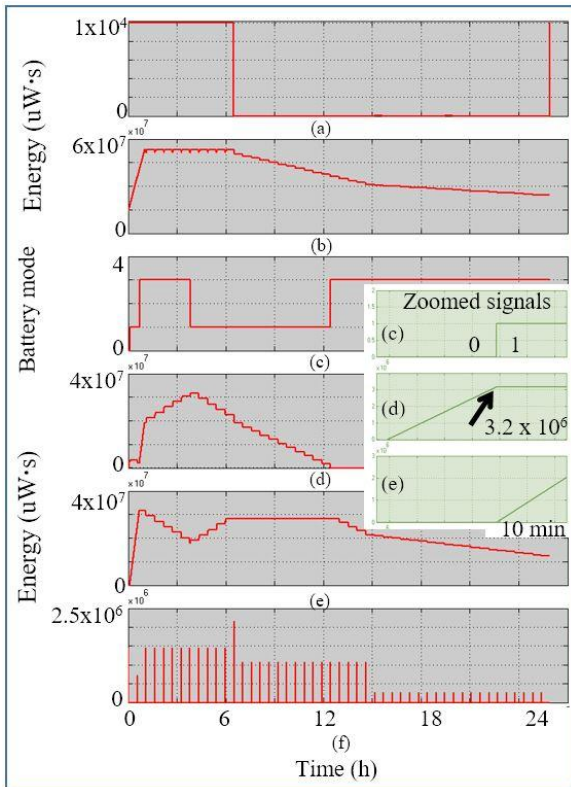


Figure 11. Simulation results of the battery control, (a) received external energy, (b) stored energy in batteries, (c) battery mode, (d) stored energy in battery 1, (e) stored energy in battery 2, and (f) energy distributed to the AnalogFrontEnd

First, we changed the battery mode only when one battery was fully charged, regardless of the status of the other battery. During the simulation, we modified the battery control scheme. When one battery was empty and the other was charged up to 10% of maximum capacity, as shown in figure 11, the battery mode was changed. This reduced the off time of the entire controller. The model therefore enables the designers to specify efficient managing methods through the simulation.

IV. CONCLUSION

This paper proposed a system level hybrid functional and power modeling methodology to extend the longevity of implantable seizure controllers. This model divided a seizure controller into several sub-blocks according to their function. The sub-blocks were reclassified into energy source, energy consumer, and power manager depending on the role of

energy in the controllers. The energy sources, including **PowerGenerator**, and the energy consumers, including The MonitoringElectrode, the AnalogFrontEnd, the SeizureDetector, the Stimulator, the StimulatingElectrode and the **WirelessCommunicator**, had information about the rate and quantity of energy, which was generated and consumed, respectively. The power manager dynamically distributes energy according to current events and expected events as well as remaining energy. The designed model for implantable seizure controller described both the functional operation and power management based on its operation. Consequently, this model supported predicting the behaviors of each sub-block as well as an entire system, analyzing the power generation and consumption together, and managing power dynamically. It enables system designers to consider system specifications within a given power budget at the early stage of design.

REFERENCES

1. Chung-Ping Y, Sheng-Fu L, Da-Wei C, Yi-Cheng L, Fu-Zen S, Chao-Hsien H, A Portable Wireless Online Closed-Loop Seizure Controller in Freely Moving Rats, *IEEE Transactions on Instrumentation and Measurement*, 2011, 60(3), pp. 513-521.
2. J. Carey, *Brain Facts: A Primer on the Brain and Nervous System*, 2016. [Online]. Available: <http://www.brainfacts.org/book>
3. N. C. Bhavaraju, M. G. Frei, and I. Osorio, Analog seizure detection and performance evaluation, *IEEE Transactions on Biomedical Engineering*, 2006, 53(2), pp. 238-245.
4. Epilepsy.NHS.U.K. 2014, [Online]. Available: <http://www.nhs.uk/Conditions/Epilepsy/Pages/Introduction.aspx>
5. Florian M, Ralph G. A, Christian E. E, Klaus L, Seizure prediction: the long and winding road, *Brain*, 2007, 130(2), pp. 314-333.
6. Jerome E, Timothy A P, Jean A, *Epilepsy: a comprehensive textbook vol. 3*, Lippincott Williams & Wilkins.
7. Muhammad T S, Dang K N, Mohamad S, A low-power implantable device for epileptic seizure detection and neurostimulation, *Biomedical Circuits and Systems Conference*, 2010, pp154-157.
8. Marco C, Michelangelo G, Alessandro S, Stefano G, Salvatore R, Massimo P, Enrico M, Danilo D, A Top-Down Constraint-Driven Methodology for Smart System Design, *IEEE Circuits and Systems Magazine*, 2014, 14(1), pp. 37-57.
9. Andrea C, Alessandro D, Emilio S, Mauro S, Kinetic and thermal energy harvesters for implantable medical devices and biomedical autonomous sensors, *Measurement Science and Technology*, 2014, 25(1).
10. Andreas G, Suhas C, Manan K, Parisa R, Abstract system-level models for early performance and power exploration, 17th Asia and South Pacific Design Automation Conference, 2012, pp. 213-218.
11. Saadia D, Eric S, Jean-Philippe D, Johann L, Dominique B, Model Driven High-Level Power Estimation of Embedded Operating Systems Communication Services, *International Conferences on Embedded Software and Systems*, 2009, pp. 475-481.
12. Yu X, Rijubrata B, Zhirong Y, Matti S, Petri S, Antti Y, A System-Level Model for Runtime Power Estimation on Mobile Devices, *IEEE/ACM Int'l Conference on & Int'l Conference on Cyber, Physical and Social Computing - Green Computing and Communications*, 2010, pp. 27-34.
13. Saumya C, Kanishka L, Anand R, Sujit D, Variation-Aware System-Level Power Analysis, *IEEE Transactions on Very Large Scale Integration (VLSI) Systems*, 2010, 18(8), pp. 1173-1184.
14. Qinru Q, Qing W, and Massoud P, Stochastic modeling of a power-managed system-construction and optimization, *IEEE Transactions on Computer-Aided Design of Integrated Circuits and Systems*, 2001, 20(10), pp. 1200-1217
15. MATLAB. The MathWorks, Inc. U.S.A., 2017. [Online]. Available: http://www.mathworks.com/products/matlab/?s_tid=hp_fp_ml
16. SIMULINK. The MathWorks, Inc. U.S.A., 2017. [Online] Available: <https://www.mathworks.com/products/simulink.html/>
17. Moo S, Zhi Y, Wentai L, *Microelectronics of Recording, Stimulation, and Wireless Telemetry for Neuroprosthetics: Design and Optimization*, Implantable Neural Prostheses 2, Springer New York, pp. 253-330.
18. Xiaodan Z, Lei L, Jia H C, Lei Y, Peng L, Ming-Yuan C, Wang

- L G, Ramamoorthy R, Gavin S D, Kuang-Wei C, Minkyu J, A 100-Channel 1-mW Implantable Neural Recording IC, IEEE Transactions on Circuits and Systems I: Regular Papers, 2013, 60(10), pp. 2584-2596.
19. My E M A Y, Mohamad S, Claude T, A neuromimetic ultra low-power ADC for bio-sensing applications," Joint IEEE North-East Workshop on Circuits and Systems and TAISA Conference, 2009, pp. 1-4.
 20. Koushaeian L, Ghafari B, Goodarzi F, Evans R, Skafidas E, Design considerations for low-power ADC for retinal prosthesis applications, 7th International Conference on Broadband Communications and Biomedical Applications, 2011, pp. 232-235.
 21. Shulyzki R, Abdelhalim K, Bagheri A, Florez C M, Carlen P L, Genov R, 256-site active neural probe and 64-channel responsive cortical stimulator," IEEE Custom Integrated Circuits Conference, 2011, pp. 1-4.
 22. Wei-Ming C, Herming C, Tsan-Jieh C, Chia-Lun H, Chi J, Ming-Dou K, Chun-Yu L, Ya-Chun H, Chia-Wei C, Tsun-Yuan F, Ming-Seng C, Yue-Loong H, Sheng-Fu L, Yu-Lin W, Fu-Zen S, Yu-Hsing H, Chia-Hsiang Y, Chung-Yu W, A Fully Integrated 8-Channel Closed-Loop Neural-Prosthetic CMOS SoC for Real-Time Epileptic Seizure Control, IEEE Journal of Solid-State Circuits, 2014, 49(1), pp. 232-247.
 23. Ruslana S, Karim A, Arezu B, M. Tariqus Salam, Carlos M F, Jose L P V, Peter L C, Roman G, 320-Channel Active Probe for High-Resolution Neuromonitoring and Responsive Neurostimulation, IEEE Transactions on Biomedical Circuits and Systems, 2015, 9(1), pp. 34-49.
 24. Muhammad T S, Mohamad S, Dang K N, A novel low-power-implantable epileptic seizure-onset detector, IEEE Transactions on Biomedical Circuits and Systems, 2011, 5(6), pp. 568-578.
 25. Sourabh R, Randy C, Low complexity algorithms for heart rate and epileptic seizure detection, 2nd International Symposium on Applied Sciences in Biomedical and Communication Technologies, 2009, pp. 1-5.
 26. Srinivasa R S, Michael D, Srinivas L, Seok-Jun L, Raúl B, Jay M, Samer G, Yu-Hung L, Rami A, Prashant S, Manish G, Microwatt embedded processor platform for medical system-on-chip applications, IEEE Journal of Solid-State Circuits, 2011, 46(4), pp. 721-730.
 27. Xiaoyin L, Hongwei H, Linchang Y, Luming L, Jianguo Z, Anchao Y, Yu M, Epileptic seizure detection with the local field potential of anterior thalamic of rats aiming at real time application Annual International Conference of the IEEE Engineering in Medicine and Biology Society, 2011, pp. 6781-6784.
 28. Osorio I, Frei M G, Wilkinson S B, Real-time automated detection and quantitative analysis of seizures and short-term prediction of clinical onset, Epilepsia, 1998, 39(6), pp. 615-627.
 29. Meysam A, David J G, Scott B, Randolph J N, Pedram M, A Battery-Powered Activity-Dependent Intracortical Microstimulation IC for Brain-Machine-Brain Interface, IEEE Journal of Solid-State Circuits, 2011, 46(4), pp. 731-745.
 30. Shuo C, Ying J, Yuan R, David P A, An Active Voltage Doubling AC/DC Converter for Low-Voltage Energy Harvesting Applications, IEEE Transactions on Power Electronics, 2011, 26(8).
 31. Yuan R, David P A, An Input-Powered Active AC/DC Converter with Zero Standby Power for Energy Harvesting Applications, IEEE Energy Conversion Congress and Exposition, 2010, pp. 4441 - 4446.
 32. Naser K P, Stefano F, François K, Maher K, An ultra-low power li-ion battery charger for micro-power solar energy harvesting applications, 19th IEEE International Conference on Electronics, Circuits, and Systems, 2012, pp. 516-519.
 33. Thilini W, Nihal K, D Alistair S R, An extra-low-frequency RS-SCALDO technique: A new approach to design voltage regulator modules, IEEE Applied Power Electronics Conference and Exposition, 2015, pp. 2039-2043.
 34. Pei-Chen W, Yi-Ping K, Chung-Shiang W, Ching-Te C, Yuan-Hua C, Wei H, PVT-aware digital controlled voltage regulator design for ultra-low-power (ULP) DVFS systems, 27th IEEE International System-on-Chip Conference, 2014, pp. 136-139.
 35. THINERGY® MEC202. Infinite Power Solutions, 2012, [Online]. Available:
<http://media.digikey.com/pdf/Data%20Sheets/Infinite%20Power%20Solutions%20PDFs/MEC202.pdf>